Geophysical Research Letters

RESEARCH LETTER
10.1029/2021GL094817

Key Points:

- Active boulder falls identified in a near-equatorial impact crater on Mars
- Timing of most significant activity refined to a period of just over one Earth year
- Local geology and crater age likely important, but not only, causes of boulder activity

Supporting Information:

Supporting Information may be found in the online version of this article.

Correspondence to:

P. M. Grindrod,
p.grindrod@nhm.ac.uk

Citation:

Grindrod, P. M., Davis, J. M., Conway, S. J., & de Haas, T. (2021). Active boulder falls in Terra Sirenum, Mars: Constraints on timing and causes. *Geophysical Research Letters*, *48*, e2021GL094817. https://doi.org/10.1029/2021GL094817

Received 15 JUN 2021
Accepted 23 SEP 2021

Active Boulder Falls in Terra Sirenum, Mars: Constraints on Timing and Causes

Peter M. Grindrod[1], Joel M. Davis[1], Susan J. Conway[2], and Tjalling de Haas[3]

[1]Department of Earth Sciences, Natural History Museum, London, UK, [2]Laboratoire de Planétologie et Géodynamique, Nantes, France, [3]Department of Physical Geography, Universiteit Utrecht, Utrecht, The Netherlands

Abstract We use time series images to identify significant active boulder falls in an impact crater on Mars. Evidence for active boulder falls include boulder trails with impact marks from bouncing and rolling, and dark patches from boulder impacts away from the base of the crater walls. We were able to define three time periods with active boulder falls and additional slope streak formation, for which we refined the most significant activity to a time period between January 2012 and March 2013. A search of 236 images within 500 km of the study site identified two further sites with similar, but reduced, activity during the same time period. We discuss plausible mechanisms for the boulder fall activity, and conclude that the local geology and crater age is likely to be of significant importance. Our method of identifying and highlighting such activity will allow further studies of active surface processes on Mars.

Plain Language Summary Mars has active surface processes, driven by environmental effects and meteorite impacts. But can interior processes cause changes at the surface today? Answering this question will help expand the recent discoveries of marsquakes by NASA's InSight lander, by identifying possible regions of seismic activity on the planet. Here we use time series orbital images to identify significant boulder falls in a crater on Mars. The temporal resolution of different cameras allows us to refine the timing of the most significant change to a time period of within just over an Earth year. Searching all similar images within 500 km revealed two further sites with similar, but reduced, activity within the same time period. Although our results do not rule out exogenic processes, the concurrent activity in several sites at similar times offers evidence of possibly related causes of boulder fall activity.

1. Introduction

The last decade has seen significant improvements in the identification and monitoring of active surface processes on Mars. Repeat observations have allowed the study of a wide range of features and processes. Many of these studies have concentrated on changes observed on the slopes of crater walls, particularly of gully (e.g., Dundas et al., 2015) and recurring slope lineae (RSL) features (e.g., McEwen et al., 2014). To date, none of these active features have been driven by endogenic processes, with environmental conditions instead the most likely explanation for change. Some of the most significant changes involving boulder movement have been identified at high latitudes on Mars, where a number of environmental processes are likely enhanced (Dundas et al., 2019). To date, such significant boulder movement has not been studied in detail at lower latitudes on Mars.

On Earth, boulder size and fall frequency have been used as proxies for earthquake location (e.g., Keefer, 1984). On Mars, this correlation has been applied to studies of boulder populations in the graben of Cerberus Fossae (Brown & Roberts, 2019; Roberts et al., 2012), in addition to proposed evidence of recent, localized seismic activity in Valles Marineris, and Jezero Crater (Senthil Kumar et al., 2019; Sinha et al., 2020). However, these studies were restricted to images representing a single time period, and thus no active boulder transport was identified. Here we use repeat orbital images to study significant active boulder transport in an unnamed near-equatorial crater in Terra Sirenum (Figure 1). Dark flows on the crater walls are made mostly of meter-scale boulders, and through a rigorous co-registration procedure, we have identified several areas of active boulder transport, and discuss possible causes for the activity.

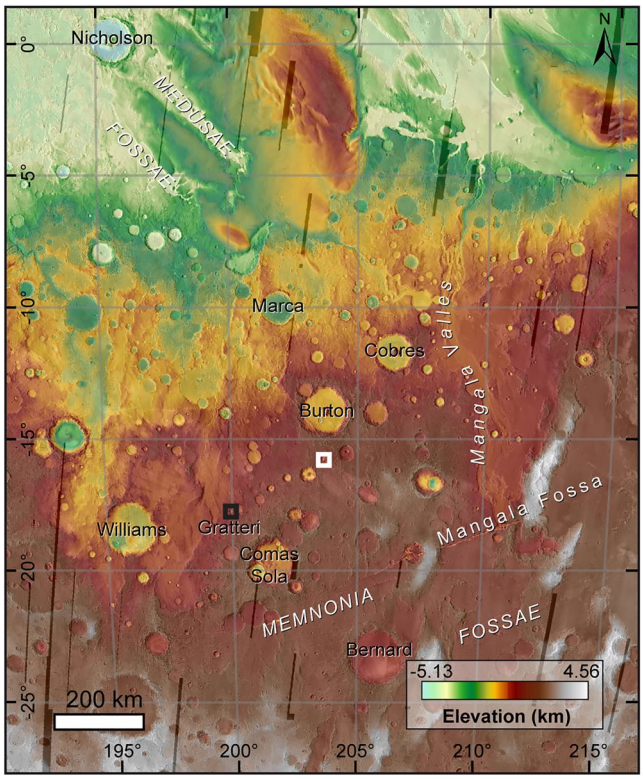

Figure 1. Regional context of the study site. Named craters are labeled in black, other notable features in white. The main study site, and location for Figure 2, is marked by the white box. Secondary study site, and Figure S3 in Supporting Information S1, is marked by the black box. Background image is Thermal Emission Imaging System daytime infrared image (Christensen et al., 2004) overlain by Mars Orbiter Laser Altimeter elevation (Smith et al., 2001).

2. Study Site

The study area (Figure 2) is a ~9 km diameter crater (−15.7°, 203.6°), that sits within a larger ~25 km diameter crater in Terra Sirenum. The study crater is ~900 m deep, with a central peak that is 300 m above the crater floor, and inner walls that have a typical maximum slope of ~40–45°. The crater has a noticeable sub-circular shape, and in the north of the crater, rim collapse has created an internal landslide deposit and caused wall retreat of up to ~500 m. Dark deposits on the majority of the internal wall slopes of the crater can be observed in Mars Reconnaissance Orbiter Context Camera (CTX, Malin et al., 2007) images, which in High Resolution Imaging Science Experiment (HiRISE, McEwen et al., 2007) images can be resolved as being composed of meter-scale boulders (Figure 2). These deposits appear relatively young, with no apparent effect from aeolian modification (e.g., bedforms such as ripples, transverse aeolian ridges, or dunes) or impact craters. These deposits appear to be the most recent geomorphological features in this crater. The possibility of recent surface change at this crater is emphasized by regions that appear to be relatively dust-free (Figure 2) in Colour and Stereo Surface Imaging System (CaSSIS) images (N. Thomas et al., 2017).

3. Data and Methods

With the exception of CaSSIS images, all data were acquired through the NASA Planetary Data System (PDS) and combined in a Geographical Data System to aid analysis and interpretation. CaSSIS data are available through the ESA Planetary Science Archive (PSA). We used repeat CTX and HiRISE images of the study region, which cover over 10 Earth years. We followed standard stereo Digital Terrain Model (DTM) and image co-registration procedures (Kirk, 2003; Kirk et al., 2008). This process resulted in DTMs with spatial resolutions of 20 m/px and 1 m/px, and orthoimages of 6 m/px and 0.25 m/px for CTX and HiRISE images, respectively. As of May 2021, there were eight repeat CTX images covering the target crater (Table S1 in Supporting Information S1). As of May 2021, there were 10 repeat HiRISE images covering the target crater, with five in the west, and five in the east (Table S1 in Supporting Information S1). We created HiRISE stereo DTMs of both sets, and co-registered and orthorectified the relevant images. To identify and highlight changes, we subtracted images in time order to create a "relative change" image. Prior to subtraction, orthoimages were normalized to produce images of similar brightness, with formal image calibration into reflectance data unnecessary for change detection (Parsons & Miyamoto, 2018). We used elevation data from the Mars Global Surveyor MOLA for global context (~463 m/px), and Mars Express HRSC (100 m/px, Gwinner et al., 2016) for regional context. We also used infrared mosaics of Mars Odyssey Thermal Emission Imaging System images (100 m/px) for global context. The CaSSIS image we used was a 4.5 m/px two-color product, with band centers (and bandwidths) of BLU = 499.9 (118.0), and PAN = 675.0 (229.4) (N. Thomas et al., 2017). We used a synthetic CaSSIS RGB color image, with channels of PAN, NIR, and "synthetic blue," respectively (Tornabene et al., 2017). To search for regional rockfalls, we analyzed all 236 HiRISE image observations taken before September 2020 within a 500 km radius of the study site (Table S2 in Supporting Information S1). In addition, we marked those HiRISE images that had slope streaks present and used the image acquisition date to note whether new slope streaks formed between dates that correlated with the timing of boulder transport in the study site. We also marked the location of those HiRISE images that contained likely new impacts, using earlier CTX images to bracket the possible impact date.

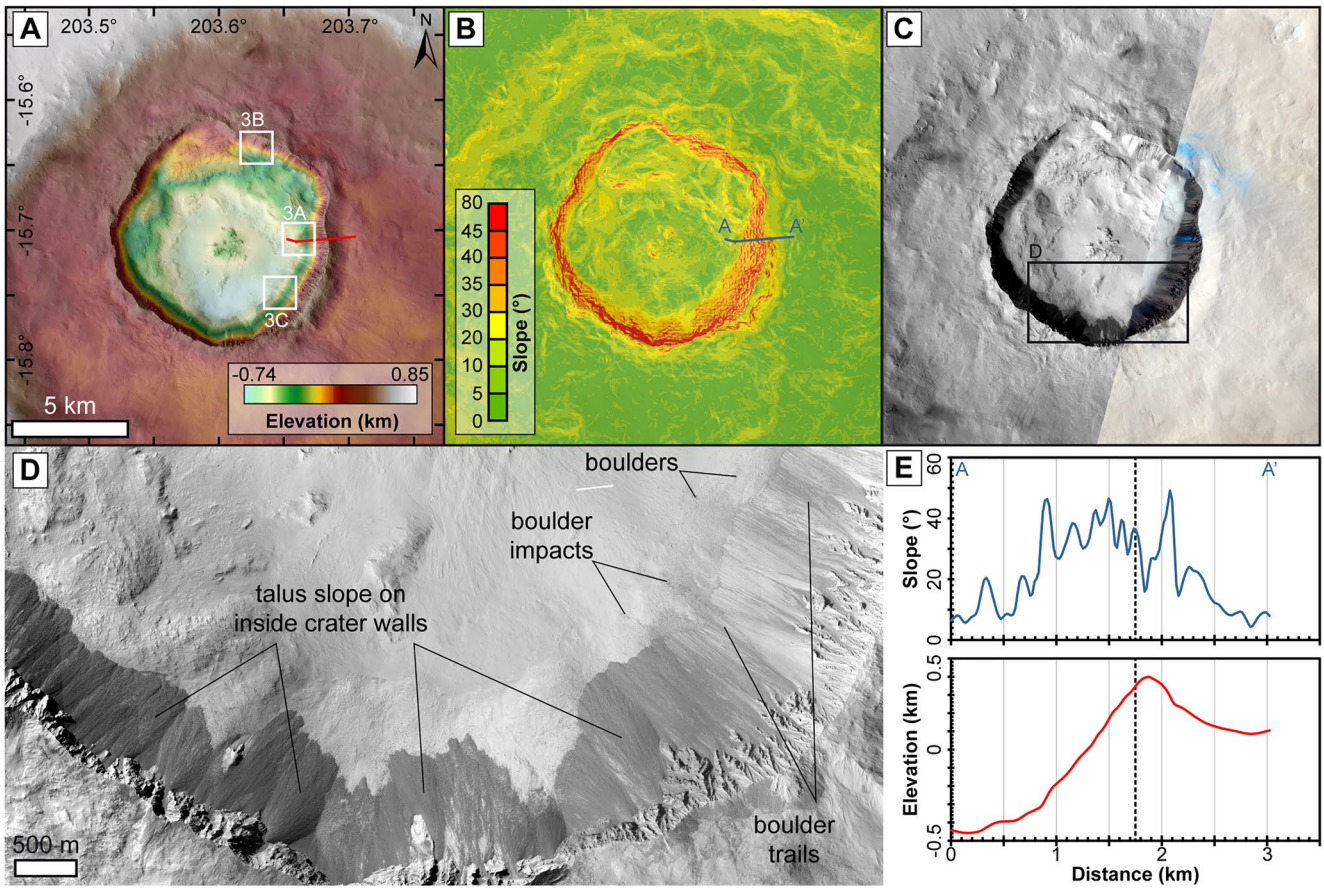

Figure 2. Local context of the study site. (a) The height of the study crater, with Context Camera (CTX) image D10_031260_1641 overlain by CTX stereo Digital Terrain Model (DTM) elevation. Also shown are the locations of subsequent figures (white boxes) and elevation profile (red line). (b) The CTX DTM slope of the study crater. Blue line shows slope profile location. (c) CTX image overlain by Colour and Stereo Surface Imaging System image MY34_003772_343. Subsequent figure shown by black box. (d) Mosaic of High Resolution Imaging Science Experiment images ESP_024825_1640 (left) and PSP_004110_1640 (right) showing the typical distribution of boulder deposits. (e) Elevation (bottom) and slope (top) profiles across the eastern crater wall in the location of significant boulder movement. Dashed line shows the source location of active boulders in this location.

4. Results

4.1. Change Details

Surface changes were identified with the relative change images, before confirmation or rejection through "blinking" the before and after images. The use of HiRISE images allowed us to separate changes due to boulder falls (source region change, boulder trails, boulder impacts) from other change features such as slope streaks and possible RSL. Examples of typical changes due to boulder falls are shown in Figures 3, S1 and S2 in Supporting Information S1. All 23 boulder changes occur on the internal crater walls and consist of one or more of the following features: dark boulder trails, sometimes with individual impacts from boulder bouncing, imprinted into the regolith on the slopes; dark patches at and away from the base of the wall slope due to boulder impact. In most cases, multiple boulder trails and impacts occur, and are likely evidence of at least several boulders having been transported during this time period in that particular location. In most cases, it was not possible to identify a newly deposited boulder responsible for these changes, with multiple impact patches likely caused by single boulders. In those few cases where a new boulder was identified beyond the final impact patch, typical long axis lengths were ~1–2 m. For those seven changes for which a likely source region could be identified, vertical fall heights ranged from ~355 to 856 m (mean = 631 m; SD = 183 m), over horizontal distances of ~586–1,456 m (mean = 1,039 m; SD = 349 m), giving runout efficiencies (ratio between horizontal and vertical distance) of 1.44–1.90 (mean = 1.64; SD = 0.2). Separate to our change detection study, we identified 438 clear occurrences of static boulders that lay at the end of

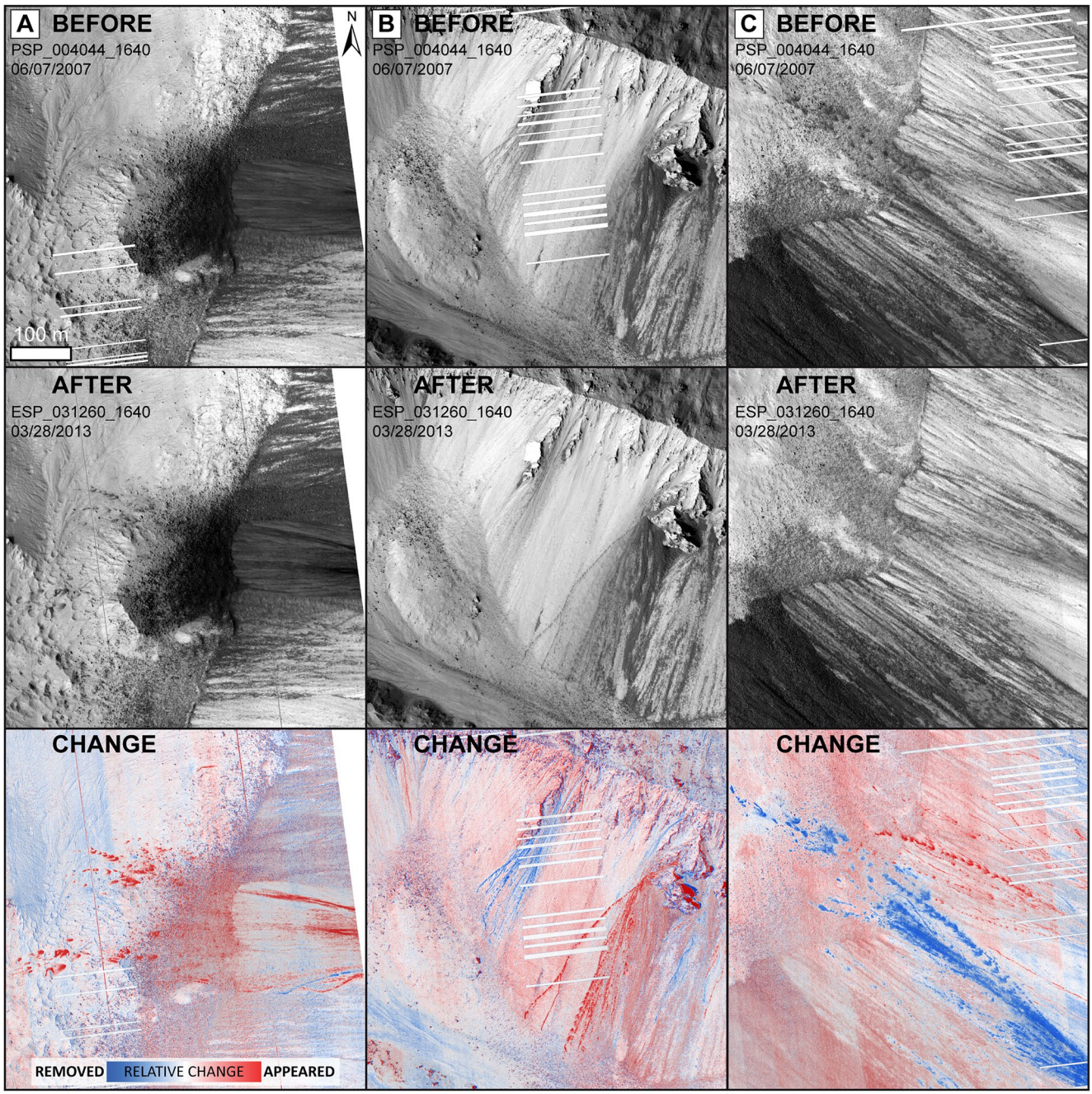

Figure 3. Examples of boulder movement as seen in High Resolution Imaging Science Experiment images. In each case, top is before movement, middle is after movement, and bottom is the relative change. The locations of (A), (B), (C) are shown in Figure 2.

existing trails, beyond the talus slopes. These boulders varied in their long axis length from ~1.2 to 13.2 m (mean = 3.6 m; SD = 1.5 m). Complete HiRISE orthoimage coverage was restricted on the western- and eastern-most crater wall slopes, but the spatial density of these boulders was greatest on the southern crater wall slope. Also evident were boulder trails and impact patches that faded in appearance, becoming lighter, between images. Although different imaging parameters preclude quantitative analysis, we observe that even the largest dark boulder trails and impact patches have almost completely faded within 7 Earth years. Larger boulder events do however leave a topographic signature in the regolith that persists. The majority of slope streaks were restricted to the interior slopes of the study crater, with only occasional occurrences close to the base of the internal crater wall slopes and active boulder movement, limiting the possible number of

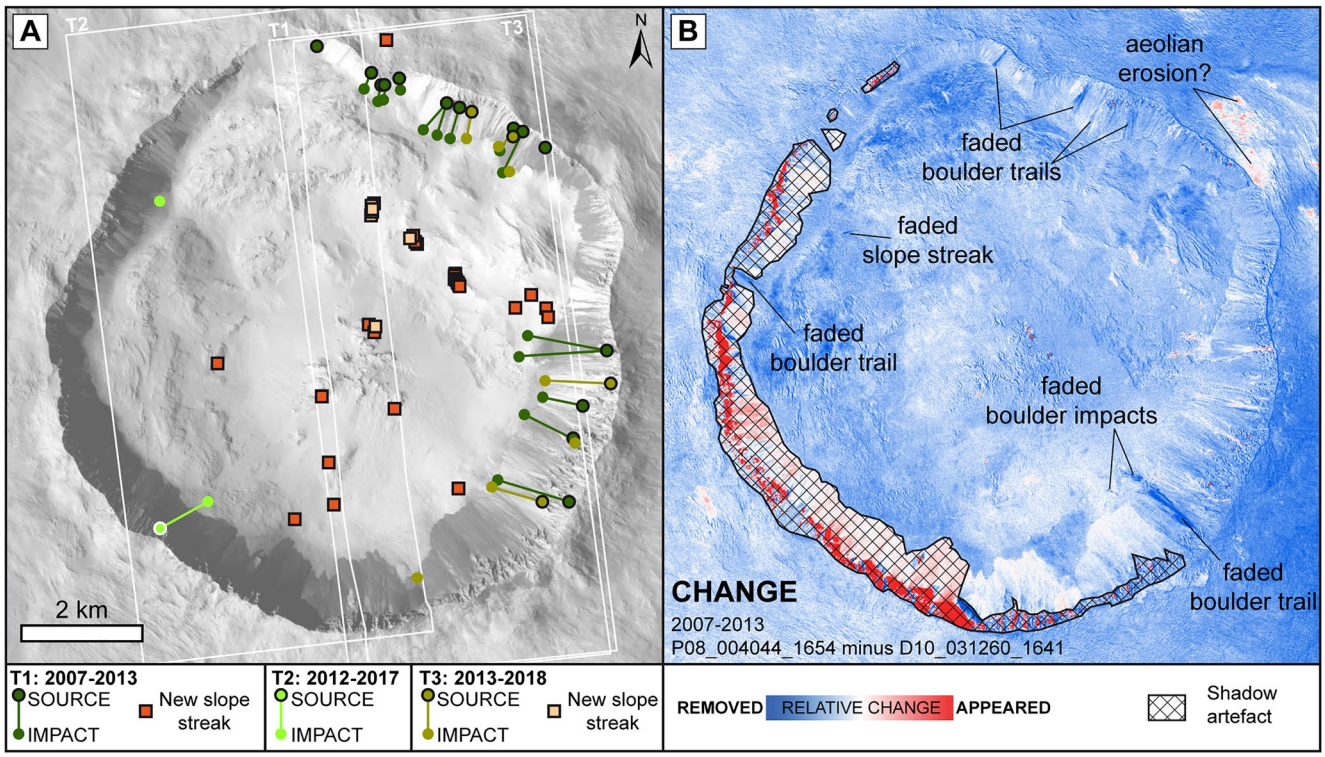

Figure 4. Summary of changes at the study site. (a) Boulder movement and new slope streaks over two time periods made using High Resolution Imaging Science Experiment (extent shown by white boxes) and Context Camera (CTX) data. Base image is CTX image D10_031260_1641. (b) Relative change as seen in CTX, used to refine time of changes.

direct joint occurrences (Chuang et al., 2007). The slope streaks faded at a similar rate to the boulder-related dark features.

4.2. Change Timing

The repeat HiRISE images allowed us to define three different time periods of change (Figures 4 and S6 in Supporting Information S1): (T1) 2,116 days between June 12, 2007 and March 28, 2013, covering the east of the crater, (T2) 1,989 days between January 7, 2012 and June 18, 2017, covering the west of the crater, and (T3) 2,029 days between March 28, 2013 and October 17, 2018, covering the east of the crater again. During T1, at least 14 areas of significant boulder impact patches and trails were observed, in addition to 25 new slope streaks. During T2, two areas of minor boulder impact patches were observed, and no slope streaks. During T3, six significant areas of boulder impact patches were observed, as well as seven new slope streaks. The use of CTX images helped refine the timing of the most significant events due to the increase in temporal resolution and areal coverage, although the smallest changes are difficult to observe due to the reduced spatial resolution (Figure 4). Therefore, using CTX images, the T1 changes can be refined to a time period of just 452 days between January 1, 2012 and March 28, 2013. The minor events of T2 and events of T3 could not be refined further due to their small size and a lack of additional time series images.

4.3. Regional Changes

In the regional HiRISE image study, we identified only one area of active boulder falls, in Gratteri Crater. To catalog all possible active surface changes, we identified 73 images with slope streaks, and 21 images with possible new impact events (Figure 5). Slope streaks are more abundant to the northeast of the regional study region, and less abundant to the southwest. Given that the appearance of slope streaks likely diminishes relatively quickly, we used the acquisition date of each image to determine whether a slope streak was present during the CTX-refined T1 time period. Of those 29 images taken during this time period, 11 had

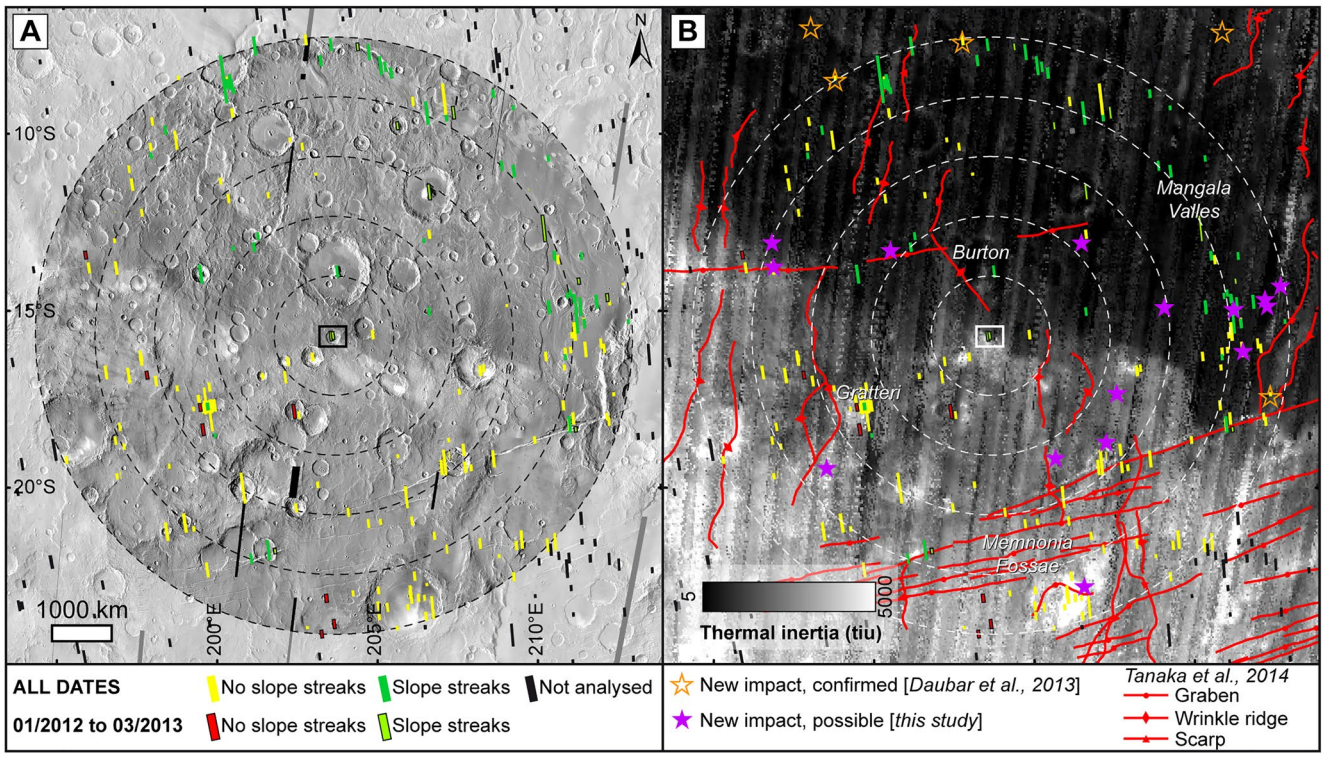

Figure 5. Regional High Resolution Imaging Science Experiment image change search, including slope streaks (colored boxes) and possible new impacts (stars). (a) Results of the slope streak investigation, overlain on Thermal Emission Imaging System daytime infrared image. (b) Results of the possible new impacts investigation, showing impacts previously confirmed (hollow orange stars, Daubar et al., 2013), and unconfirmed impacts identified in this study (filled purple stars). Background image is TES thermal inertia values (Putzig & Mellon, 2007). Also shown are regional tectonic features (Tanaka et al., 2014). In both figures, dashed circles mark 100 km radii from the study site.

slope streaks, 10 of which were to the northeast and east of the regional study area, whereas 8 did not have slope streaks, all located to the west, southwest, and south of the regional study area.

5. Discussion

Our study site is ~235 km northeast from the 6.9 km diameter Gratteri impact crater, which is one of the youngest, large craters on Mars, and is the only regional site at which we identified active boulder falls. Although ages derived from crater size-frequency studies produce a range of possible impact ages for Gratteri, it is likely that this impact event happened <5 Ma, and almost certainly <20 Ma (Hartmann et al., 2010). Active mass wasting processes, including boulder transport (Figure S3 in Supporting Information S1), have been previously identified in Gratteri crater (M. F. Thomas et al., 2020). Just like Gratteri crater, our study site also contains pitted material, likely to be impact melt (Tornabene et al., 2012). Together, these two craters reinforce discussion of the possible causes of the activity. We consider four main causes that could be responsible for the active boulder transport.

The presence of a distinct lithological layer, such as impact melt, which is susceptible to mass wasting when oversteepened, is the most likely requisite for boulder transport. This cause explains the boulder material forming talus slopes on the walls inside the majority of the crater, as well as limited boulder occurrence on the outer crater walls (Figure S4 in Supporting Information S1). The source region slope of ~36° for the largest boulder event is greater than the approximate critical angle of 32° suggested as necessary for rockfalls on Mars (Tesson et al., 2020). A contiguous layer between our study site and Gratteri crater would outcrop in other craters, which we do not observe, but a similar local layer could also account for boulder activity in Gratteri crater. The color information in CaSSIS images support this idea, with "blue" boulders appearing to originate at a layer of bedrock of similar color ~100 m below the crater rim. Similar color arguments have been made for boulder and possible source layers at Gratteri Crater (M. F. Thomas et al., 2020).

The seismic triggering of mass wasting matches well with terrestrial experience, especially boulder falls related to earthquakes. There are many examples of boulder size and transport properties being used in studies of earthquakes (e.g., Anooshehpoor et al., 2004; Brune, 1996; Brune et al., 2007), although rockfalls alone do not imply seismicity. Seismic triggering would likely occur in combination with the geology, where susceptible lithologies undergo constant small mass wasting events, punctuated by larger events due to marsquakes. The timing of the most significant boulder changes in our study site fall within the same broader time period as the most significant boulder events in Gratteri crater (M. F. Thomas et al., 2020). However, there is a lack of supporting evidence. The InSight instruments are unlikely to detect an event at such distance (Banerdt et al., 2020), and none of the nearest faults appear young. One possible exception is a graben ~380 km to the SSW of our study site that contains boulders, boulder trails, and slope streaks (Figure S5 in Supporting Information S1). Also, given the separation distance, a marsquake would require a magnitude of greater than ~7–8 (Keefer, 1984), which would likely cause other surface changes that we do not observe. The presence of talus cones at both boulder fall sites, indicators of repeat falls, suggests a coincidence of timing, but does not rule out separate, localized seismic events.

Similar to most other feature changes on Mars, environmental processes could be responsible. The main such processes that could contribute are solar insolation-induced thermal stress or seasonal frost, as suggested at other rockfall sites on Mars (Sinha et al., 2020; Tesson et al., 2020). But we would expect more widespread boulder transport in other craters at these latitudes, the geology (e.g., a susceptible lithology) is also important. Boulder transport in our study regions is not confined to equator-facing slopes, as observed by Tesson et al. (2020) at this latitude, and the location is outside the typical latitude range where frost has been observed (e.g., Schorghofer & Edgett, 2006), reducing the likely importance of thermal effects. Aeolian erosion could also lead to crater wall retreat and boulder fall (e.g., Grant et al., 2008; Sinha et al., 2020), although, again, geology would have to be invoked to explain the localized activity. The relative effectiveness of such a mechanism over a relatively short period of time is unknown (e.g., Williams et al., 2020), but backweathering rates are likely higher in young craters, but decreasing over time (de Haas et al., 2015). The backweathering rates of our main study crater is likely similar to that derived for Gratteri Crater, of between ~0.005 and 0.01 mm year^{-1} (de Haas et al., 2015), which correspond to distances of 25–50 m and 100–200 m over 5 and 20 Ma, respectively. These backweathering rates are an order of magnitude higher than Amazonian erosion rates (Golombek et al., 2014), due to the oversteepened and highly fractured crater walls (de Haas et al., 2015), but still lower than required to produce the sub-circular shape of our study impact crater, suggesting that (a) boulder falls increase the backweathering rates beyond those of standard alcove processes, and (b) boulder fall activity also likely decreases over time at impact craters.

New impacts have been identified as a cause of slope streaks on Mars (e.g., Burleigh et al., 2012; Chuang et al., 2007) and are capable of causing a local seismic effect (Daubar et al., 2020). However, no new impacts have been identified in or close to our study site, nor near those sites of high latitude boulder movements (Dundas et al., 2019). In general, the regional distribution of slope streaks can be directly related to the dust abundance at the surface, as revealed by the correlation with areas of low thermal inertia (Figure 5). The only three sites outside of dusty areas that have slope streaks that are present within the refined time period of significant change are our study site, Gratteri crater, and the SSW graben with boulders.

6. Conclusions

Although the possible causes of active boulder transport are unlikely to be mutually exclusive (e.g., Dundas et al., 2019), the local geology in the study crater, and other active sites, is likely to be a significant factor in controlling whether active boulder falls occur on Mars. We are unable to rule out endogenic causes such as marsquakes, and the concurrence with other boulder falls offers tantalizing evidence of possible related events. However, other environmental processes such as thermal stress, and/or aeolian erosion, are likely to be ongoing, widespread, and concurrent. Although there is incomplete regional image coverage, it seems unlikely that new impacts are responsible for the activity. Our method of stereo DTM generation and time series orthoimage analysis offers a robust way of identifying and highlighting such activity, and will allow further studies of a range of active surface processes on Mars.

Data Availability Statement

Standard data products are available from the NASA PDS Imaging Node (https://pds-imaging.jpl.nasa.gov/) and the ESA PSA (http://archives.esac.esa.int/psa/#!Table%20View/CaSSIS=instrument). Derived data products are available at https://doi.org/10.6084/m9.figshare.14687160.

Acknowledgments
Peter M. Grindrod and Joel M. Davis acknowledge support from the UK Space Agency (grants ST/R002355/1, ST/V002678/1). Susan J. Conway acknowledges support from CNES. CaSSIS is a project of the University of Bern and funded through the Swiss Space Office via ESA's PRODEX programme. The instrument hardware development was also supported by the Italian Space Agency (ASI) via the ASI-INAF agreement no. 2020-17-HH.0, the INAF/Astronomical Observatory of Padova, and the Space Research Center (CBK) in Warsaw. Support from SGF (Budapest), the University of Arizona (Lunar and Planetary Laboratory) and NASA are also gratefully acknowledged. Operations support from Charlotte Marriner, funded by the UK Space Agency (grants ST/R003025/1, ST/V002295/1) is also recognized. The authors thank two anonymous reviewers, and editor Andrew Dombard, for insightful comments.

References

Anooshehpoor, A., Brune, J. N., & Zeng, Y. (2004). Methodology for obtaining constraints on ground motion from precariously balanced rocks. *Bulletin of the Seismological Society of America*, *94*(1), 285–303. https://doi.org/10.1785/0120020242

Banerdt, W. B., Smrekar, S. E., Banfield, D., Giardini, D., Golombek, M., Johnson, C. L., et al. (2020). Initial results from the InSight mission on Mars. *Nature Geoscience*, *13*(3), 183–189. https://doi.org/10.1038/s41561-020-0544-y

Brown, J. R., & Roberts, G. P. (2019). Possible evidence for variation in magnitude for marsquakes from fallen boulder populations, Grjota Valles, Mars. *Journal of Geophysical Research: Planets*, *124*(3), 801–822. https://doi.org/10.1029/2018JE005622

Brune, J. N. (1996). Precariously balanced rocks and ground-motion maps for Southern California. *Bulletin of the Seismological Society of America*, *86*(1A), 43–54. https://doi.org/10.1785/bssa08601a0043

Brune, J. N., Purvance, M. D., & Anooshehpoor, A. (2007). Gauging earthquake hazards with precariously balanced rocks: Finding easily toppled boulders that are still standing provides a way to test models of seismic hazard. *American Scientist*, *95*(1), 36–43. https://doi.org/10.1511/2007.63.36

Burleigh, K. J., Melosh, H. J., Tornabene, L. L., Ivanov, B., McEwen, A. S., & Daubar, I. J. (2012). Impact airblast triggers dust avalanches on Mars. *Icarus*, *217*(1), 194–201. https://doi.org/10.1016/j.icarus.2011.10.026

Christensen, P., Jakosky, B. M., Kieffer, H. H., Malin, M. C., McSween, H. Y., Jr., Nealson, K., et al. (2004). The Thermal Emission Imaging System (THEMIS) for the Mars 2001 Odyssey mission. *Space Science Reviews*, *110*(1–2), 85–130. https://doi.org/10.1023/B:SPAC.0000021008.16305.94

Chuang, F. C., Beyer, R. A., McEwen, A. S., & Thomson, B. J. (2007). HiRISE observations of slope streaks on Mars. *Geophysical Research Letters*, *34*(20). https://doi.org/10.1029/2007GL031111

Daubar, I. J., Lognonné, P., Teanby, N. A., Collins, G. S., Clinton, J., Stähler, S., et al. (2020). A new crater near InSight: Implications for seismic impact detectability on Mars. *Journal of Geophysical Research: Planets*, *125*(8), e2020JE006382. https://doi.org/10.1029/2020JE006382

Daubar, I. J., McEwen, A. S., Byrne, S., Kennedy, M. R., & Ivanov, B. (2013). The current martian cratering rate. *Icarus*, *225*(1), 506–516. https://doi.org/10.1016/j.icarus.2013.04.009

de Haas, T., Conway, S. J., & Krautblatter, M. (2015). Recent (Late Amazonian) enhanced backweathering rates on Mars: Paracratering evidence from gully alcoves. *Journal of Geophysical Research: Planets*, *120*(12), 2169–2189. https://doi.org/10.1002/2015JE004915

Dundas, C. M., Diniega, S., & McEwen, A. S. (2015). Long-term monitoring of martian gully formation and evolution with MRO/HiRISE. *Icarus*, *251*, 244–263. https://doi.org/10.1016/j.icarus.2014.05.013

Dundas, C. M., Mellon, M. T., Conway, S. J., & Gastineau, R. (2019). Active boulder movement at high martian latitudes. *Geophysical Research Letters*, *46*(10), 5075–5082. https://doi.org/10.1029/2019GL082293

Golombek, M. P., Warner, N. H., Ganti, V., Lamb, M. P., Parker, T. J., Fergason, R. L., & Sullivan, R. (2014). Small crater modification on Meridiani Planum and implications for erosion rates and climate change on Mars. *Journal of Geophysical Research: Planets*, *119*(12), 2522–2547. https://doi.org/10.1002/2014JE004658

Grant, J. A., Wilson, S. A., Cohen, B. A., Golombek, M. P., Geissler, P. E., Sullivan, R. J., et al. (2008). Degradation of Victoria crater, Mars. *Journal of Geophysical Research*, *113*(E11). https://doi.org/10.1029/2008JE003155

Gwinner, K., Jaumann, R., Hauber, E., Hoffmann, H., Heipke, C., Oberst, J., et al. (2016). The High Resolution Stereo Camera (HRSC) of Mars Express and its approach to science analysis and mapping for Mars and its satellites. *Planetary and Space Science*, *126*, 93–138. https://doi.org/10.1016/j.pss.2016.02.014

Hartmann, W. K., Quantin, C., Werner, S. C., & Popova, O. (2010). Do young martian ray craters have ages consistent with the crater count system? *Icarus*, *208*(2), 621–635. https://doi.org/10.1016/j.icarus.2010.03.030

Keefer, D. K. (1984). Landslides caused by earthquakes. *Geological Society of America Bulletin*, *95*, 406. https://doi.org/10.1130/0016-7606(1984)95<406:Lcbe>2.0.Co;2

Kirk, R. L., Howington-Kraus, E., Redding, B., Galuszka, D., Hare, T. M., Archinal, B. A., et al. (2003). High-resolution topomapping of candidate MER landing sites with Mars Orbiter Camera narrow-angle images. *Journal of Geophysical Research*, *108*(E12). https://doi.org/10.1029/2003je002131

Kirk, R. L., Howington-Kraus, E., Rosiek, M. R., Anderson, J. A., Archinal, B. A., Becker, K. J., et al. (2008). Ultrahigh resolution topographic mapping of Mars with MRO HiRISE stereo images: Meter-scale slopes of candidate Phoenix landing sites. *Journal of Geophysical Research*, *113*. https://doi.org/10.1029/2007je003000

Malin, M. C., Bell, J. F., Cantor, B. A., Caplinger, M. A., Calvin, W. M., Clancy, R. T., et al. (2007). Context Camera investigation on board the Mars Reconnaissance Orbiter. *Journal of Geophysical Research*, *112*(E5). https://doi.org/10.1029/2006JE002808

McEwen, A. S., Dundas, C. M., Mattson, S. S., Toigo, A. D., Ojha, L., Wray, J. J., et al. (2014). Recurring slope lineae in equatorial regions of Mars. *Nature Geoscience*, *7*(1), 53–58. https://doi.org/10.1038/ngeo2014

McEwen, A. S., Eliason, E. M., Bergstrom, J. W., Bridges, N. T., Hansen, C. J., Delamere, W. A., et al. (2007). Mars Reconnaissance Orbiter's High Resolution Imaging Science Experiment (HiRISE). *Journal of Geophysical Research*, *112*(E5), E05S02. https://doi.org/10.1029/2005JE002605

Parsons, R., & Miyamoto, H. (2018). Optimizing change detection for planetary remote sensing datasets. *Journal of Physics: Conference Series*, *1036*, 012004. https://doi.org/10.1088/1742-6596/1036/1/012004

Putzig, N. E., & Mellon, M. T. (2007). Apparent thermal inertia and the surface heterogeneity of Mars. *Icarus*, *191*(1), 68–94. https://doi.org/10.1016/j.icarus.2007.05.013

Roberts, G. P., Matthews, B., Bristow, C., Guerrieri, L., & Vetterlein, J. (2012). Possible evidence of paleomarsquakes from fallen boulder populations, Cerberus Fossae, Mars. *Journal of Geophysical Research*, *117*(E2). https://doi.org/10.1029/2011je003816

Schorghofer, N., & Edgett, K. S. (2006). Seasonal surface frost at low latitudes on Mars. *Icarus*, *180*(2), 321–334. https://doi.org/10.1016/j.icarus.2005.08.022

Senthil Kumar, P., Krishna, N., Prasanna Lakshmi, K. J., Raghukanth, S. T. G., Dhabu, A., & Platz, T. (2019). Recent seismicity in Valles Marineris, Mars: Insights from young faults, landslides, boulder falls and possible mud volcanoes. *Earth and Planetary Science Letters*, *505*, 51–64. https://doi.org/10.1016/j.epsl.2018.10.008

Sinha, R. K., Rani, A., Conway, S. J., Vijayan, S., Basu Sarbadhikari, A., Massé, M., et al. (2020). Boulder fall activity in the Jezero crater, Mars. *Geophysical Research Letters*, *47*(23), e2020GL090362. https://doi.org/10.1029/2020GL090362

Smith, D. E., Zuber, M. T., Frey, H. V., Garvin, J. B., Head, J. W., Muhleman, D. O., et al. (2001). Mars Orbiter Laser Altimeter: Experiment summary after the first year of global mapping of Mars. *Journal of Geophysical Research*, *106*(E10), 23689–23722. https://doi.org/10.1029/2000JE001364

Tanaka, K. L., Robbins, S. J., Fortezzo, C. M., Skinner, J. A., & Hare, T. M. (2014). The digital global geologic map of Mars: Chronostratigraphic ages, topographic and crater morphologic characteristics, and updated resurfacing history. *Planetary and Space Science*, *95*, 11–24. https://doi.org/10.1016/j.pss.2013.03.006

Tesson, P. A., Conway, S. J., Mangold, N., Ciazela, J., Lewis, S. R., & Mège, D. (2020). Evidence for thermal-stress-induced rockfalls on Mars impact crater slopes. *Icarus*, *342*, 113503. https://doi.org/10.1016/j.icarus.2019.113503

Thomas, M. F., McEwen, A. S., & Dundas, C. M. (2020). Present-day mass wasting in sulfate-rich sediments in the equatorial regions of Mars. *Icarus*, *342*, 113566. https://doi.org/10.1016/j.icarus.2019.113566

Thomas, N., Cremonese, G., Ziethe, R., Gerber, M., Brändli, M., Bruno, G., et al. (2017). The Colour and Stereo Surface Imaging System (CaSSIS) for the ExoMars Trace Gas Orbiter. *Space Science Reviews*, *212*(3), 1897–1944. https://doi.org/10.1007/s11214-017-0421-1

Tornabene, L. L., Osinski, G. R., McEwen, A. S., Boyce, J. M., Bray, V. J., Caudill, C. M., et al. (2012). Widespread crater-related pitted materials on Mars: Further evidence for the role of target volatiles during the impact process. *Icarus*, *220*(2), 348–368. https://doi.org/10.1016/j.icarus.2012.05.022

Tornabene, L. L., Seelos, F. P., Pommerol, A., Thomas, N., Caudill, C. M., Becerra, P., et al. (2017). Image simulation and assessment of the colour and spatial capabilities of the Colour and Stereo Surface Imaging System (CaSSIS) on the ExoMars Trace Gas Orbiter. *Space Science Reviews*, *214*(1), 18. https://doi.org/10.1007/s11214-017-0436-7

Williams, J., Day, M., Chojnacki, M., & Rice, M. (2020). Scarp orientation in regions of active aeolian erosion on Mars. *Icarus*, *335*, 113384. https://doi.org/10.1016/j.icarus.2019.07.018